Article

Synthesis and Fundamental Studies of (HGe)SiH Molecules: Precursors to Semiconductor Hetero- and Nanostructures on Si

Cole J. Ritter, Changwu Hu, Andrew V. G. Chizmeshya, John Tolle, Douglas Klewer, Ignatius S. T. Tsong, and John Kouvetakis

J. Am. Chem. Soc., **2005**, 127 (27), 9855-9864• DOI: 10.1021/ja051411o • Publication Date (Web): 16 June 2005

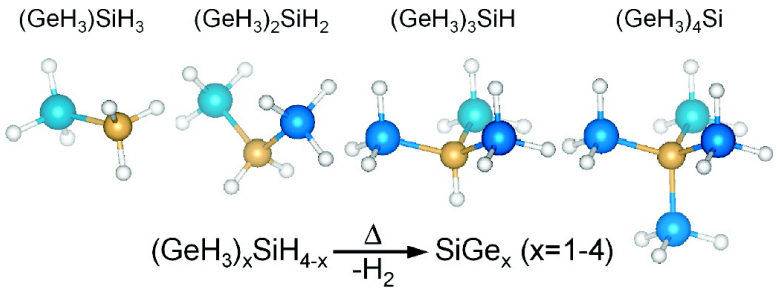

More About This Article

Additional resources and features associated with this article are available within the HTML version:

- Supporting Information
- Links to the 4 articles that cite this article, as of the time of this article download
- Access to high resolution figures
- Links to articles and content related to this article
- Copyright permission to reproduce figures and/or text from this article

View the Full Text HTML

J|A|C|S
ARTICLES
Published on Web 06/16/2005

Synthesis and Fundamental Studies of $(H_3Ge)_xSiH_{4-x}$ Molecules: Precursors to Semiconductor Hetero- and Nanostructures on Si

Cole J. Ritter,[†] Changwu Hu,[‡] Andrew V. G. Chizmeshya,[§] John Tolle,[†] Douglas Klewer,[†] Ignatius S. T. Tsong,[‡] and John Kouvetakis*,[†]

Contribution from the Department of Chemistry and Biochemistry, Department of Physics and Astronomy, and Center for Solid State Science, Arizona State University, Tempe, Arizona, 85287

Received March 4, 2005; E-mail: jkouvetakis@asu.edu

Abstract: The synthesis of the entire silyl−germyl sequence of molecules $(H_3Ge)_xSiH_{4-x}$ ($x = 1-4$) has been demonstrated. These include the previously unknown $(H_3Ge)_2SiH_2$, $(H_3Ge)_3SiH$, and $(H_3Ge)_4Si$ species as well as the H_3GeSiH_3 analogue which is obtained in practical high-purity yields as a viable alternative to disilane and digermane for semiconductor applications. The molecules are characterized by FTIR, multinuclear NMR, mass spectrometry, and Rutherford backscattering. The structural, thermochemical, and vibrational properties are studied using density functional theory. A detailed comparison of the experimental and theoretical data is used to corroborate the synthesis of specific molecular structures. The $(H_3Ge)_xSiH_{4-x}$ family of compounds described here is not only of intrinsic molecular interest but also provides a unique route to a new class of Si-based semiconductors including epitaxial layers and coherent islands (quantum dots), with Ge-rich stoichiometries SiGe, $SiGe_2$, $SiGe_3$, and $SiGe_4$ reflecting the Si/Ge content of the corresponding precursor. The layers grow directly on Si(100) at unprecedented low temperatures of 300−450 °C and display homogeneous compositional and strain profiles, low threading defect densities, and atomically planar surfaces circumventing entirely the need for conventional graded compositions or lift-off technologies. The activation energies of all Si−Ge hydride reactions on Si(100) ($E_a \approx 1.5-2.0$ eV) indicate high reactivity profiles with respect to H_2 desorption, consistent with the low growth temperatures of the films. The quantum dots are obtained exclusively at higher temperatures ($T > 500$ °C) and represent a new family of Ge-rich compositions with narrow size distribution, defect-free microstructures, and homogeneous, precisely tuned elemental content at the atomic level.

Introduction

Silicon plays a ubiquitous role in modern semiconductor materials technology development. Consequently, most new device structures based on any other semiconductors grown on Si typically rely on sophisticated integration schemes. From a materials science perspective, integration of thermally and dimensionally dissimilar systems with Si is highly nontrivial since the interface structures must withstand thermal and mechanical stresses during the fabrication process without degrading desired electrical characteristics. Si_xGe_{1-x} alloys on Si represent an example of such a system, which is of significant current interest. Until very recently, work on $Si/Si_{1-x}Ge_x$ heterostructures has concentrated almost exclusively on growth of Si-rich concentrations (Ge < 30 atom %) due to applications in high-frequency electronic devices.[1−3] The Ge-rich analogues are much less developed despite their great potential in future generations of optoelectronic devices such as multiple quantum well structures for detection and emission of mid to long wavelength IR radiation.[2] In addition, Ge-rich $Si_{1-x}Ge_x$ alloys serve as virtual substrates and buffer layers for growth of tensile-stressed Si with enhanced carrier mobilities and for the monolithic integration of optical III−V semiconductors with Si electronics.[4] For effective device performance, the $Si_{1-x}Ge_x$ films on Si must be uniformly stressed or fully relaxed thin layers that display smooth surface morphology and low dislocation densities.[5] However, conventional growth on Si is complicated by the inherent lattice mismatch between the films and the substrate, which produces copious dislocations, strain nonuniformities, and high surface roughness. Thus, one of the ongoing materials challenges is to develop suitable methods based on low-temperature pathways to prepare device quality Ge-rich layers on Si.

One approach to integration in the Si−Ge system involves the growth of thick graded buffer layers in which the germanium content is gradually increased up to 100% Ge. In this case, the misfit strain between the Si substrate and the Si−Ge film is gradually relieved with increasing film thickness.[4,6] Approximately 10 μm is required to achieve acceptable levels of

[†] Department of Chemistry and Biochemistry.
[‡] Department of Physics and Astronomy.
[§] Center for Solid State Science.

(1) Meyerson, B. S. *IBM J. Res. Dev.* **2000**, *44*, 391−407.
(2) Mooney, P. M.; Chu, J. O. *Annu. Rev. Mater. Sci.* **2000**, *30*, 355−362.
(3) Tromp, R. M.; Ross, F. M. *Annu. Rev. Mater. Sci.* **2000**, *30*, 431−449.
(4) Currie, M. T.; Samavedam, S. B.; Langdo, T. A.; Leitz, C. W.; Fitzgerald, E. A. *Appl. Phys. Lett.* **1998**, *72*, 1718−1720.
(5) Lee, M. L.; Pirreta, A. J.; Fitzgerald, E. A. *J. Vac. Sci. Technol., B* **2004**, *22*, 158−164.

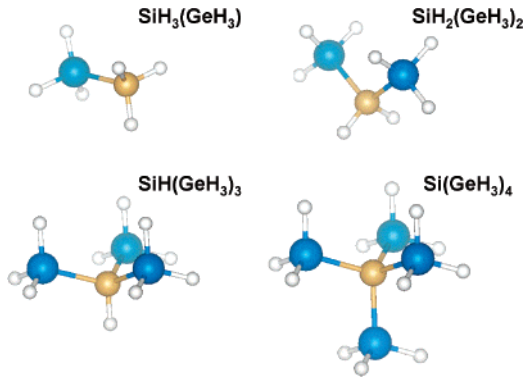

Figure 1. Structures of the molecular precursors $(H_3Ge)_xSiH_{4-x}$ ($x = 1-4$). Legend: Si (yellow), Ge (blue), H (white). These structures are derived from analytical and spectroscopic data and are confirmed by first principle simulations.

threading dislocation densities (as low as $\sim 10^6$ cm^{-2}), and a chemical mechanical polishing (CMP) step is necessary to produce a smooth surface prior to subsequent growth of the active device layer. The resulting extreme film thickness and the complicated CMP step make processing of the devices very expensive and in some cases even create additional problems such as degradation of key film properties. A more straightforward approach, which obviates the need for thick films and their associated processing issues, is therefore highly desirable.

Our work in this area is focused on development of new approaches for growth of device quality SiGe materials with high Ge contents directly on Si. Our strategy is based on the preparation of single-source hydrides with direct Si−Ge bonds such as H_3GeSiH_3, $(H_3Ge)_2SiH_2$, $(H_3Ge)_3SiH$, and $(H_3Ge)_4Si$. These are obtained in viable high-purity yields via straightforward synthetic methodologies and possess the necessary high volatility and facile reactivity to serve as low-temperature (300−450 °C) precursors for growth of binary Si−Ge alloys and ternary Si−Ge−Sn semiconductors.

In this article we describe synthesis, characterization, and properties of mixed Si−Ge hydrides with the general formula $(H_3Ge)_xSiH_{4-x}$ ($x = 1-4$) (Figure 1). In particular, the $(H_3Ge)_2SiH_2$, $(H_3Ge)_3SiH$, and $(H_3Ge)_4Si$ species have been isolated and fully characterized for the first time. We have also synthesized the well-known H_3GeSiH_3 gaseous analogue in practical high purity yields as a viable alternative to the commercial sources disilane, trisilane, and digermane for industrial and research applications.[7−9] Earlier work in this family of compounds, via silent electric discharge of SiH_4 and GeH_4 mixtures, has reported a series of isomers with Ge_2SiH_8 and Si_2GeH_8 concentrations.[10] The Ge_2SiH_8 species was identified to be almost exclusively the asymmetric isomer $(H_3Ge)GeH_2(SiH_3)$ of the $(H_3Ge)_2SiH_2$ compound. Several related formulas have appeared in the literature, including $SiGeH_6$, Si_2GeH_8, Si_3GeH_{10}, Si_4GeH_{12}, $Si_2Ge_2H_{10}$, and $SiGe_2H_8$.[9,11−13] However, these were never isolated as pure products, and their molecular structures were not assigned. They were purportedly obtained as mixtures from alloy hydrolysis and were identified by gas chromatography analysis. In addition, the isolation and full characterization of $(H_3Ge)_4Si$ has remained elusive, to the best of our knowledge. Previous attempts have not provided definitive proof of its existence as a pure product possessing the correct stoichiometry and structure.[14] One recent report in particular indicates that the molecule might not be stable for steric reasons and decomposes rapidly via evolution of digermane at or near room temperature.[15] Nevertheless, we have prepared $(H_3Ge)_4Si$ as a volatile, colorless liquid and have shown that it is in fact remarkably stable at ambient conditions and thereby suitable for materials synthesis applications. The simplicity of $(H_3Ge)_xSiH_{4-x}$ species—typical examples of classical inorganic compounds—and their high reactivity driven by elimination of extremely stable H_2 to form useful semiconductors are potentially appealing from both a fundamental and a practical viewpoint.

In this report, we also demonstrate the utility of this class of compounds to grow Si−Ge materials including heterostructures and novel nanostructures directly on Si at extraordinarily low temperatures. Initial experiments at 300−450 °C have yielded monocrystalline films possessing atomically smooth surfaces, low threading defect densities, and most importantly concentrations that match precisely the Si/Ge ratio of the corresponding precursors. In addition, we have shown that these compounds allow tuning of the film morphology by the adjustment of a single parameter (i.e., the growth temperature). At temperatures of 500−600 °C we produce almost exclusively highly coherent quantum dots rather than continuous films. A distinct and important advantage of our new method over conventional routes is the precise control of morphology, tunable composition, structure, and strain via the incorporation of the *entire* Si/Ge framework of the gaseous precursor into both layers and quantum dots. The layers are of much higher quality than those obtained using conventional sources, circumventing entirely the need for graded compositions or lift-off technologies. The quantum dots represent a new family of Ge-rich compositions with enormous potential in optoelectronic applications based entirely on Si technologies. A major limitation of quantum dot growth by conventional methods based on bimolecular reactions of silanes and germanes is that compositional variations exist among dots. This problem is also completely resolved with the single source approach in which the Si−Ge concentration in the dot reflects exactly the Si−Ge content of the precursor. In addition, we have found that our low-temperature route eliminates interdiffusion at the film/substrate interface, which is particularly problematic for growth of pure Ge dots on Si.

Results and Discussion

The syntheses of $(H_3Ge)_2SiH_2$ and $(H_3Ge)_3SiH$ utilize low-temperature reactions of $KGeH_3$ with triflate- and perfluoroalkylsulfonyloxy-substituted silanes such as $H_xSi(SO_3CF_3)_{4-x}$ and $H_xSi(SO_3C_4F_9)_{4-x}$ ($x = 1, 2, 3$), respectively, in suitable solvents. In each case, the solvents were selected to obtain the

(6) Mooney, P. M.; Jordan-Sweet, J. L.; Ismail, K.; Chu, J. O.; Feenstra, R. M.; LeGoues, F. K. *Appl. Phys. Lett.* **1995**, *67*, 2373−2375.
(7) Lobreyer, T.; Oeler, J.; Sundermeyer, W. *Chem. Ber.* **1991**, *124*, 2405−2410.
(8) Varma, R.; Cox, A. P. *Angew. Chem.* **1962**, *76*, 649; *Angew. Chem., Int. Ed. Engl.* **1964**, *3*, 586.
(9) Feiselmann, B. F.; Bridgewater, N. J. (Solarex Co.). U.S. Patent 4,777,023, Feb. 18, 1986, Oct. 11, 1988.
(10) Mackay, K. M.; Hosfield, S. T.; Stobart, S. R. *J. Chem. Soc. A* **1969**, 2937−2943.
(11) Phillips, C. S. G.; Powell, P.; Semlyen, J. A.; Timms, P. L. *Z. Anal. Chem.* **1963**, 202−211.
(12) Timms, P. L.; Phillips, C. S. G. *Inorg. Chem.* **1964**, *3*, 606−607.
(13) Phillips, C. S. G.; Timms, P. L. *Anal. Chem.* **1963**, *35*, 505−510.
(14) Dutton, W.; Onyszchuk, M. *Inorg. Chem.* **1968**, *7*, 1735−1739.
(15) Foster, S. P.; Leung, K.-F.; Mackay, K. M.; Thomson, R. A. *Aust. J. Chem.* **1986**, *39*, 1089−1099.

desired solubility of the reactants and to allow a convenient and effective separation and purification of the products from the solvent medium.

$$H_xSiR_{4-x} + (4-x)KGeH_3 \rightarrow SiH_x(H_3Ge)_{4-x} + (4-x)KR \quad (1)$$

$$R = SO_3CF_3,\ SO_3C_4F_9$$

The starting materials $H_xSi(SO_3CF_3)_{4-x}$ and $H_xSi(SO_3C_4F_9)_{4-x}$ ($x = 1, 2$) were prepared (the latter for the first time) in nearly quantitative, high-purity yields via reactions of the corresponding phenylsilanes and the appropriate sulfonic acids (eq 2).

$$H_xSi(C_6H_5)_{4-x} + HR \rightarrow H_xSiR_{4-x} + xC_6H_6 \quad (2)$$

These compounds were fully characterized by spectroscopic methods, including FTIR, multinuclear NMR, as well as C, H, and F elemental analysis. The triflate (SO_3CF_3) derivative is more common and less expensive and thereby more feasible for process scale-up. However, the $-SO_3C_4F_9$ compounds provide substantially higher product yields especially in the higher-order Ge-rich products. We therefore explored both routes to assess their relative benefits. Details of the compound syntheses, purification, and characterizations are provided in the Experimental Section. The H_3GeSiH_3 compound has been previously synthesized using a variety of routes including the use of $H_3Si(SO_3C_4F_9)$ as starting material.[7] However, in all cases the yields were relatively low with respect to conversion of the germane source to be viable for semiconductor development applications. Here we employ the simple single-step method described below, under optimized conditions, to prepare semiconductor-grade product in 35−40% yield using the inexpensive triflate reagent (eq 3).

$$H_3Si(SO_3CF_3) + KGeH_3 \rightarrow H_3GeSiH_3 + K(SO_3CF_3) \quad (3)$$

Finally, our synthesis of $(H_3Ge)_4Si$ utilized reactions involving the mixed halide triflate $Cl_2Si(SO_3CF_3)_2$ and $KGeH_3$ as the source of the germyl ligand. The product was obtained in modest but sufficient quantities to conduct a complete characterization of the compound and grow $SiGe_4$ films by gas source MBE as described below. Recently, the synthesis of the analogous $(SiH_3)_4Ge$ species and its derivatives $(SiH_3)_2GeH_2$ and $(SiH_3)_3GeH$ has been reported.[16] Our preparation of $(H_3Ge)_2SiH_2$, $(H_3Ge)_3SiH$, and $(H_3Ge)_4Si$ described here, therefore, completes a broad family of mixed Si−Ge tetrahedral hydrides with formulas $(H_3Ge)_xSiH_{4-x}$ and $(SiH_3)_xGeH_{4-x}$, respectively.

(a) $(H_3Ge)_2SiH_2$. The $(H_3Ge)_2SiH_2$ product is obtained in high yields (60%) as a colorless, air-sensitive, and volatile liquid with a vapor pressure of 55 Torr at 22 °C. $(H_3Ge)_2SiH_2$ is thermally robust and appears to be less reactive in air than H_3GeSiH_3 and related silanes that are known to react explosively with oxygen. The high vapor pressure and good thermal stability indicate that $(H_3Ge)_2SiH_2$ is suitable for CVD applications. This compound also appears to possess higher stability than the well-known homonuclear analogues such as trisilane, $(H_3Si)_2SiH_2$, and digermane, H_3GeGeH_3, which are commonly used in the fabrication of Si-based devices. Thus, $(H_3Ge)_2SiH_2$ offers the possibility of becoming a safer and more efficient alternative to these compounds in synthetic materials science. $(H_3Ge)_2SiH_2$ is readily identified and characterized by its IR, NMR, and mass spectra. Its IR spectrum is relatively simple, showing two sharp absorptions at 2152 and 2074 cm^{-1}, which are assigned to the Si−H and Ge−H stretching modes, respectively. These assignments are consistent with those made previously for H_3GeSiH_3.[17] The intensity of the Ge−H peak in the spectrum is significantly stronger than the Si−H peak in accordance with the higher number of Ge−H bonds relative to Si−H bonds in the molecule. Other prominent absorptions at 805 and 702 cm^{-1} are attributed to Si−H and Ge−H bending modes, respectively. A weak band at 324 cm^{-1} corresponds to the skeletal Si−Ge stretching mode. A more detailed interpretation of the full IR spectrum is obtained from quantum chemical calculations, and it is described below. The mass spectrum of the compound displays a well-defined isotopic envelope for ($SiGe_2H_8^+$). The ^1H NMR spectra show a triplet centered at 3.11 ppm (δ Ge−H) due to GeH_3 moieties and a septet at 3.39 ppm (δ Si−H) due to SiH_2. The HMQC spectrum shows a correlation between the ^1H resonance at 3.11 ppm (δ Ge−H) and the ^{29}Si resonance at −102.45 ppm. The NMR data collectively point to a $(H_3Ge)_2SiH_2$ structure in which a central SiH_2 group is bonded with two terminal GeH_3 moieties. The integrated Ge−H/Si−H proton ratio is 3:1, as expected. The NMR frequencies correlate well with H_3GeSiH_3 (Table 1) and the related $(H_3Ge)_3SiH$ and $(H_3Ge)_4Si$ described below.

Table 1. ^1H and ^{29}Si NMR[a] Data for Polysubstituted Silylgermanes

compd	^1H, δ	^{29}Si, δ	ref
H_3GeSiH_3[b]	3.52 (q, Si*H*$_3$) 3.18 (q, Ge*H*$_3$)	−91.60	7
H_3GeSiH_3[a]	3.40 (q, Si*H*$_3$) 3.06 (q, Ge*H*$_3$)	−96.20	this work
$(H_3Ge)_2SiH_2$	3.39 (sept, Si*H*$_2$) 3.11 (t, Ge*H*$_3$)	−102.45	this work
$(H_3Ge)_3SiH$	3.41 (dect, Si*H*) 3.29 (d,Ge*H*$_3$)	−112.73	this work
$(H_3Ge)_4Si$	3.44 (s, Ge*H*$_3$)	−127.61	this work

[a] $CDCl_3$ solution. [b] C_7D_8 solution.

We also prepared $(H_3Ge)_2SiH_2$ via an alternative two-step process as a possible route to higher yields. As shown below, we initially synthesized and isolated the monosubstituted $H_3GeSiH_2(SO_3CF_3)$ compound by reactions of $PhSiH_2GeH_3$ with HSO_3CF_3 in the absence of solvent at −35 °C (eq 4). Subsequent reactions of $H_3GeSiH_2(SO_3CF_3)$ with $KGeH_3$ affords the disubstituted $(H_3Ge)_2SiH_2$ product (eq 5).

$$PhSiH_2GeH_3 + HSO_3CF_3 \rightarrow H_3GeSiH_2(SO_3CF_3) + C_6H_6 \quad (4)$$

$$H_3GeSiH_2(SO_3CF_3) + KGeH_3 \rightarrow (H_3Ge)_2SiH_2 + KSO_3CF_3 \quad (5)$$

The intermediate $H_3GeSiH_2(SO_3CF_3)$ species is isolated for the first time as a colorless, low-volatility liquid (vp = 3 Torr at 22 °C) at 72% yield. The product remains thermally stable when stored at −25 °C but decomposes slowly at 22 °C to give H_3GeSiH_3 and an unidentified residue. The compound was characterized by gas-phase IR, NMR (^1H, ^{13}C, ^{19}F), and mass spectrometry, and the data are consistent with the proposed $H_3GeSiH_2SO_3CF_3$ molecular structure (see Experimental Section for details).

(16) Lobreyer, T.; Oberhammer, H.; Sundermeyer, W. *Angew. Chem.* **1993**, *105*, 587−588.

(17) Lannon, J. A.; Weiss, G. S.; Nixon, E. R. *Spectrochim. Acta, Part A* **1970**, *26*, 221−233.

(b) $(H_3Ge)_3SiH$. Pure $(H_3Ge)_3SiH$ is obtained in ~30% yields as a colorless, air-sensitive, and volatile liquid with a vapor pressure of 10 Torr at 22 °C. Extensive NMR, mass spectrometric, and IR characterizations indicated that the molecular structure comprised a central Si atom that is bonded to three GeH_3 and one H groups similar to isobutane. In particular, the ^1H NMR spectra showed a deciplet at 3.41 ppm and a doublet at 3.29 ppm corresponding to the Si−H and Ge−H protons, respectively. The splitting patterns of the Si−H and Ge−H resonances and their corresponding integrated peak ratio of 1:9 are consistent with the isobutane-like $(H_3Ge)_3SiH$ structure. Furthermore, the HMQC spectrum showed a correlation between the ^1H resonance at 3.29 ppm (δ Ge−H) and the ^{29}Si at −112.73 ppm. The mass spectra showed an isotopic envelop at 255−238 amu as the highest mass peak corresponding $[SiGe_3H_x]^+$. Although the molecule appears to readily lose H in the mass spectrometer, the $SiGe_3$ core is retained in the gas phase. The IR spectrum shows the characteristic Si−H and Ge−H stretching modes at 2071 and 2132 cm^{-1}, respectively, and a set of absorptions at 881, 788, and 680 cm^{-1} corresponding to bending modes. The IR spectrum for $(H_3Ge)_3SiH$ was also calculated using the B3LYP functional and the 6-311++G(2d,2p) basis set as described in the next section. A close agreement between experiment and theory was obtained.

(c) $(H_3Ge)_4Si$. Tetragermylsilane was isolated as a colorless liquid with ~1 Torr vapor pressure at 22 °C, which is similar to the reported value for $(H_3Ge)_4C$ (1−2 Torr).[18] The high symmetry of the molecule leads to an extremely simple IR spectrum, which shows absorptions at 2072 and 2062 cm^{-1} corresponding to the symmetric and asymmetric Ge−H stretches, respectively. In addition, no Si−H vibrational modes were detected by FTIR. The peak positions and relative intensities closely match the calculated spectrum (see next section for theoretical and experimental IR spectra and corresponding peak assignments). The highest peak in the mass spectrum is observed in the range of 328−318 amu. The peak position and the isotopic distribution indicate H_xGe_4Si-type species consistent with the $(GeH_3)_4Si$ tetrahedral structure. The ^1H and ^{29}Si NMR spectra show single resonances at 3.44 ppm and at −127.61 ppm, respectively. The former corresponds to the $-GeH_3$ protons. This assignment was made using HMBC experiments, which confirmed the presence of a Si nucleus bonded to GeH_3 moieties. It is interesting to note that the ^{29}Si resonance in the $(GeH_3)_xSiH_{x-4}$ family of compounds shifts monotonically upfield with increasing x (see Table 1). This trend has also been observed in the $(GeH_3)_xSi(CH_3)_{4-x}$ series in which δ ^{29}Si shifts from 0.0 ppm for $x = 0$ to −71.7 ppm for $x = 1$.[15] The successful synthesis and isolation of $(H_3Ge)_4Si$ was further corroborated by Rutherford backscattering (RBS) analysis (Figure 2) of monocrystalline films and electron energy loss (EELS) analysis of quantum dots produced by MBE via unimolecular dehydrogenation of the compound at 300 and 550 °C, respectively, according to eq 6. The analytical data in both cases indicated unequivocally a Ge_4Si composition.

$$(H_3Ge)_4Si\ (gas) \rightarrow Ge_4Si\ (film) + 6H_2\ (gas) \qquad (6)$$

Density Functional Theory Simulations of Molecular Properties. Our data indicate that we have isolated, for the first time, $(H_3Ge)_2SiH_2$ with a symmetric propane-like structure. As discussed previously, Mackay et al. have reported the asymmetric isomer $(H_3Ge)GeH_2(SiH_3)$ as well as the related $H_3Ge(SiH_2)SiH_3$ and $(H_3Si)_2GeH_2$ isomers using silent electric discharge of SiH_4 and GeH_4.[10] The absence of the symmetric $(H_3Ge)_2SiH_2$ isomer suggests that it may not be stable under the high-energy conditions of the silent electric discharge process. This is in fact borne out by explicit thermochemistry calculations (described in detail below) where it is found that the symmetric isomer is metastable with respect to its asymmetrical counterpart by a mere 4 kcal/mol.

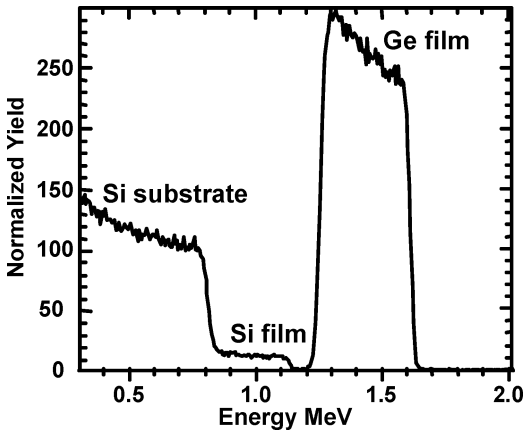

Figure 2. RBS spectrum of a 500-nm film grown via decomposition of $(H_3Ge)_4Si$ at 300 °C on Si. Simulation of the composition using the program RUMP gives exactly a 4Ge:1Si elemental ratio.

Our objective in the present study is to systematically examine the structural, energetic, and vibrational trends through the entire sequence of $SiH_{4-x}(GeH_3)_x$ molecules (e.g., $x = 1-4$), including several of the related asymmetric isomers. A discrete number of isomers exist for each member in this sequence. Digermylsilane exhibits symmetrical $(H_3Ge)_2SiH_2$ and asymmetrical $(H_3Si)GeH_2(GeH_3)$ structural isomers with skeletal ordering Ge−Si−Ge and Si−Ge−Ge, respectively. The trigermylsilane molecule possesses four configurations: two low-energy tetrahedral structures, which we refer to as $(H_3Ge)_3SiH$ and $(H_3Ge)_2GeH(SiH_3)$, and two highly metastable chainlike "$SiGe_3$" isomers, which we do not consider further here. The tetragermyl silane molecule also possesses a range of chainlike isomers; we again consider only the energetically favored symmetric case possessing Si in central tetrahedral neopentane-like coordination.

The structural, bonding, and vibrational properties of some related species, such as silane and germane, have been previously studied using a range of theoretical methods.[19−20] Disilane and digermane have also been explored, but to lesser extent. Leszczynski et al.[21] and Urban et al.[22] studied H_3GeSiH_3, using a hybrid density functional theory (DFT) based on the B3LYP exchange and correlation energy functional. It is shown that long (~2.4 Å) metal−metal bond lengths endow these molecules with unique dynamical characteristics, including weak energy barriers against SiH_3/GeH_3 rotor motion.[22] More recently,

(18) Kouvetakis, J.; Haaland, A.; Shorokhov, D. J.; Volden, H. V.; Girichev, G. V.; Sokolov, V. I.; Matsunaga, P. *J. Am. Chem. Soc.* **1998**, *120*, 6738−6744.

(19) Oberhammer, H.; Lobreyer, T.; Sundermeyer, W. *J. Mol. Struct.* **1994**, *323*, 125−128.

(20) Romero, A. H.; Kiwi, M.; Ramirez, R. *Phys. Status Solidi B* **2002**, *230*, 391−395.

(21) Leszczynski, L.; Huang, J. Q.; Schreiner, P. R.; Vacek, G.; Kapp, G.; von Ragué Schleyer, J.; Schaefer, H. F., III. *Chem. Phys. Lett.* **1995**, *244*, 252−257.

(22) Urban, J.; Schreiner, P. R.; Vacek, G.; Schleyer, P.; Huang, J. Q.; Leszczynski, J. *Chem. Phys. Lett.* **1997**, *264*, 441−448.

Table 2. Calculated Geometries for a Selection of $(H_3Ge)_xSiH_{4-x}$ Molecules with $x = 1-4$[a]

	H_3SiGeH_3	$(H_3Ge)_2SiH_2$	$SiH_3GeH_2GeH_3$	$(H_3Ge)_3SiH$	$(H_3Ge)_2GeH(SiH_3)$	$(H_3Ge)_4Si$
			Bond Lengths			
Si−Ge	2.394 (2.397)	2.397	2.398	2.401	2.401	2.404
Ge−Ge			2.445		2.450	
Si−H	1.481 (1.483)	1.484	1.482	1.487	1.482	
Ge−H	1.539 (1.536)	1.539	1.543 1.539	1.539	1.546 1.539	1.539
			Bond Angles			
Si−Ge−Ge			113.1		113.1	
Ge−Si−Ge		112.1		110.6		109.5
H−Si−H	108.7 (108.8)	108.0			110.6	
H−Ge−H	108.2 (108.3)		107.1	110.5	110.6	
H−Si−Ge	110.2 (110.1)	108.3	108.4	108.4	108.4	108.5
H−Ge−Si	110.9 (111.0)	110.7	110.8	110.8	110.9	110.6

[a] Bond lengths are listed in angstroms, and bond angles are in degrees. Values listed in parentheses for H_3GeSiH_3 were obtained using a 6-311G++(3df,2pd) basis set.

Becerra et al.[23] studied the PES of H_3GeSiH_3 using both high-level G2/MP2 and DFT methods. All of these studies established the importance of including d-type polarization functions on heavy atoms (Si,Ge) and p-type polarization functions on hydrogen atoms. Excellent agreement was found between the calculated and measured structural and vibrational properties using a 6-311G++(3df,2pd) basis set with typical bond length and frequency discrepancies on the order of 0.4 and 1.4%, respectively.

Structural and Thermochemical Trends. As a preliminary step in our study of the ground-state properties of $(H_3Ge)_xSiH_{4-x}$ molecules, we first reproduced the earlier results of Becerra et al.[23] for H_3GeSiH_3 using the high quality B3LYP/6-311G++-(3df,2pd) employed in their work. After testing several alternative basis sets, we concluded that a slight reduction in basis set size still provides an efficient and highly accurate description of molecular properties (e.g., structure trends and vibrational spectra), particularly for the heaviest members of the sequence which are more computationally demanding. Accordingly, all of our calculations were performed at the B3LYP/6-311++G-(2d,2p) basis set level as implemented in the *Gaussian03* code.[24]

The results of the structural optimizations, obtained using tight convergence criteria, are presented in Table 2. For completeness, and to compare our results with those obtained earlier by Becerra et al.,[23] we include results for the H_3GeSiH_3 molecule. For this molecule, the bond lengths obtained using a 6-311G++(2d,-2p) basis set differ by less than 0.2% from those generated at the 6-311G++(3df,2pd) level with corresponding bond angle changes on the order of several tenths of a degree. The table lists the bond length and bond angle data for six molecules: H_3GeSiH_3, the symmetrical and asymmetrical isomers of both $SiGe_2H_8$ and $SiGe_3H_{10}$, and $(H_3Ge)_4Si$. As can be seen from our data, the structural trend in the Si−Ge skeletal bonding is very simple and consists of a systematic increase in bond lengths throughout the sequence from 2.394 Å in H_3GeSiH_3 to 2.404 Å in $(H_3Ge)_4Si$. These are typical Si−Ge bonds; no stretching is observed in the central core from Si−Ge to $Si-Ge_4$. Furthermore, these values correspond closely (∼0.2%) to those in bulk Si−Ge films. The asymmetrical $(SiH_3)GeH_2(GeH_3)$ and $(H_3Ge)_2GeH(SiH_3)$ isomers display normal bulk Ge−Ge bond lengths (2.446 Å) with values 2.445 and 2.450 Å, respectively. The Si−H and Ge−H bond lengths occur as terminal groups (SiH_3,GeH_3), central SiH_2, GeH_2 moieties, or central SiH, GeH moieties. From the table it can be seen that the shortest Si−H bond lengths, 1.481 and 1.482 Å, occur in the terminal SiH_3 groups of H_3GeSiH_3 and $(SiH_3)GeH_2(GeH_3)$, respectively. A slightly longer Si−H bond length (1.484 Å) is found in the SiH_2 unit of $(H_3Ge)_2SiH_2$, while the maximal Si−H bond length 1.487 Å is associated with $(H_3Ge)_3SiH$.

Similarly, the Ge−H bond lengths of the GeH_3 ligands have a consistent value of 1.539 Å in all molecules while central Ge−H bond lengths in $(SiH_3)GeH_2(GeH_3)$ and $(H_3Ge)_2GeH(SiH_3)$ take on slightly dilated values 1.543 and 1.546 Å, respectively. The intermetallic Ge−Si−Ge skeletal bond angles vary significantly from 110.6° in $(H_3Ge)_3SiH$ to 109.5° in the $(H_3Ge)_4Si$ and 112.1° in the symmetric $(H_3Ge)_2SiH_2$ molecule. The largest skeletal intermetallic bonds occur in the asymmetrical $(H_3Si)GeH_2(GeH_3)$ and $(H_3Ge)_2GeH(SiH_3)$ molecules where the Si−Ge−Ge bond angles take on a value of 113.1°. The H−Si−H and H−Ge−H bond angles follow a more systematic trend throughout the molecular sequence. We find that the H−M−H bond angles in the terminal Si and Ge groups are in the 108.1−108.5° range (H−Ge−H and H−Si−H bond angles at the bottom and top of the range, respectively). The H−Ge−Si and H−Si−Ge bond angles are almost constant and take on average values 110.7° and 108.4°, respectively, with a variance of about 0.2° throughout the entire molecular sequence.

Table 3 lists the thermochemical energies of the molecules, including the total ground-state electronic energy E_0, the zero-point energy correction (E_{ZPE}), as well as the thermal corrections to the enthalpy (H_{CORR}) and free energy (G_{CORR}) at 298 K. The totals obtained by adding the corrections to the electronic energy are also listed in the table. A comparison of the calculated E_0 and E_{ZPE} for H_3GeSiH_3, obtained using the 6-311++G(2d,2p) and 6-311++G(3df,2pd) basis sets, with the latter shown in

(23) Becerra, R.; Boganov, S. E.; Egorov, M. P.; Faustov, V. I.; Nefedov, O. M.; Walsh, R. *Phys. Chem. Chem. Phys.* **2001**, *3*, 184−192.
(24) Frisch, M. J. et al. *Gaussian 03*; Gaussian Inc.: Pittsburgh, PA, 2003.

Table 3. Calculated Thermochemical Energies for a Selection of $(H_3Ge)_xSiH_{4-x}$ Molecules with $x = 1-4$[a]

molecule	E_0	E_{ZPE}	$E_0 + H_{CORR}$	$E_0 + G_{CORR}$
H_3SiGeH_3	−2370.13514	0.04748	−2370.08140	−2370.11559
	(−2370.14109)	(0.04739)	(−2370.08754)	(−2370.12189)
$(H_3Ge)_2SiH_2$	−4448.35457	0.06244	−4448.28454	−4448.32403
$SiH_3GeH_2GeH_3$	−4448.36041	0.06362	−4448.28772	−4448.33032
$(H_3Ge)_3SiH$	−6526.57532	0.07888	−6526.48413	−6526.53578
$(H_3Ge)_2GeH(SiH_3)$	−6526.58679	0.07941	−6526.49506	−6526.54628
$(H_3Ge)_4Si$	−8604.79645	0.09325	−8604.68837	−8604.74718

[a] Thermal corrections for zero-point energy, internal energy, enthalpy, and Gibbs free energy are listed as E_{ZPE}, E_{TOT}, H_{CORR}, and G_{CORR}, respectively. Values listed in parentheses for H_3GeSiH_3 were obtained using a 6-311G++(3df,2pd) basis set (energies in hartree).

parentheses, indicates small energetic differences of about 0.006 hartree (~20 meV/atom). All of the other calculated energies reported in Table 3 were computed using the 6-311++G-(2d,2p) basis. The total Gibbs free energy of each molecule at 298 K is obtained by adding the thermal free energy correction to the electronic ground state energy value from each column. Our calculations indicate that the asymmetrical isomers are generally slightly favored at room temperature. Specifically, for H_3GeSiH_3 the free energy difference is 0.0063 hartree (16 meV/atom), while for $(H_3Ge)_2GeH(SiH_3)$ the difference is 0.0105 hartree (20 meV/atom). Note that k_BT at 300 K ≈ 25 meV. On this basis, the symmetrical isomers that we obtained experimentally are slightly metastable compared to their asymmetric counterparts.

Vibrational Spectra. To corroborate the identification of the synthesized precursors, we simulated the infrared vibrational spectra of the symmetric $(H_3Ge)_xSiH_{4-x}$ isomers using the B3LYP DFT functional at the 6-311++G(2d,2p) basis set level. The spectra of $(H_3Ge)_2SiH_2$, $(H_3Ge)_3SiH$, and $(H_3Ge)_4Si$ are shown in Figure 3. No symmetry was imposed in the calculation of the frequency spectra, and all molecules (including H_3GeSiH_3, not shown) exhibited a positive definite spectrum of harmonic frequencies, indicating that the ground-state structures are dynamically stable. Corresponding experimental spectra are shown as negative traces in these plots. Each plot (Figure 3) shows the low-frequency nonskeletal bands (<1000 cm^{-1}) and an inset comparing the calculated and measured high-frequency spectra (Si−H and Ge−H vibrations). Scale factors of 0.98 and 0.989 were applied to the high- and low-frequency spectra, respectively. The latter value (0.989) agrees with the value found by Urban et al.[22] in their treatment of Si_2H_6, Ge_2H_6, and H_3GeSiH_3 using B3LYP density functional theory. We also calculated the IR spectrum of the asymmetric $(GeH_3)GeH_2(SiH_3)$ isomer (not shown) and found excellent agreement with the data reported previously by MacKay et al.[10]

The interpretation of the high-frequency spectral features is straightforward: the peaks designated "1" and "2" in the insets (Figure 3) are common to all molecules and are due to symmetric and anti-symmetric Ge−H stretching vibrations, respectively. But the progression is not monotonic through the molecular sequence: the scaled calculated frequencies for the $(H_3Ge)_2SiH_2$, $(GeH_3)_3SiH$, and $(H_3Ge)_4Si$ are 2054, 2067, and 2050 cm^{-1} for the symmetric Ge−H stretches and 2067, 2080, and 2067 cm^{-1} for the asymmetric counterparts. The corresponding experimental Ge−H features are 2066(2074), 2060-(2072), and 2060(2070) cm^{-1}. The mean observed splitting between features "1" and "2" of approximately 10 cm^{-1} agrees well with the computed splitting of 14 cm^{-1}. The asymmetric Si−H bands in $(H_3Ge)_2SiH_2$ and $(H_3Ge)_3SiH$ occur at slightly higher frequency. These bands are labeled "3" in the inset of

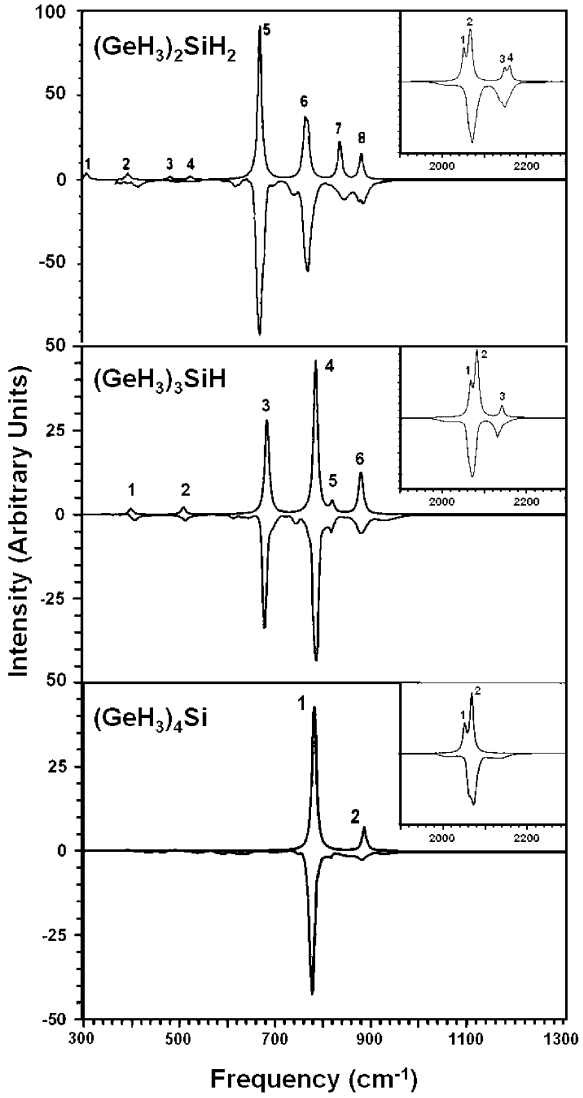

Figure 3. Calculated and observed IR spectra (upper and lower trace, respectively). Inset shows the hydrogen stretching region. The numbers labeling the various features are described in the text. Note the excellent agreement of both the vibrational frequencies and the peak intensities between the experimental and calculated spectra.

Figure 3 (top and middle). The band labeled "4" in the inset of Figure 3 (top) is associated with a symmetric vibration of the Si−H bond. No Si−H bands are present in $(H_3Ge)_4Si$.

Again, the splitting between the symmetric and anti-symmetric Si−H stretch frequencies in $(H_3Ge)_2SiH_2$ is calculated to be ~12 cm^{-1}, which is identical to the observed splitting. However, as seen from the plotted spectra the calculated separation *between* the frequency centroids of the Ge−H and Si−H bands (~89 cm^{-1}) is somewhat larger than the observed

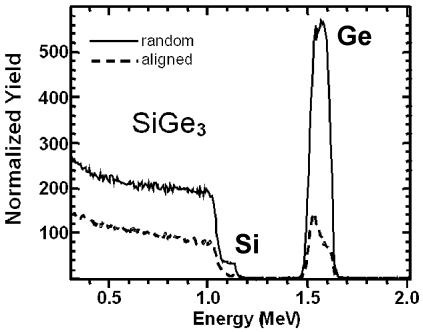

Figure 4. RBS spectra of a $SiGe_3$ film on Si(100). The sharp reduction in channeling from the film interface to the surface indicates that the defect concentration decreases across the layer.

separation of ~77 cm^{-1}. Our benchmark tests using smaller basis sets reveal that M−H bands exhibit the greatest sensitivity to basis set size. As an example we have verified, in the case of the $(H_3Ge)_2SiH_2$ IR spectrum, that the use of the 6-311++G-(3df,2pd) does not significantly improve the quality of the calculated spectrum, yielding a contraction of the calculated Ge−H, Si−H centroid spacing of only about 8 cm^{-1}.

The lower frequency nonskeletal vibrational structure is considerably more complex, but several of the most intense features are strongly correlated across the different molecules. Symmetric Ge−H wagging vibrations appear as features "6" in $(H_3Ge)_2SiH_2$ (805 cm^{-1}), "4" in $(H_3Ge)_3SiH$ (790 cm^{-1}), and "1" in $(H_3Ge)_4Si$ (782 cm^{-1}). We assign symmetric Si−H wagging to features "5" in $(H_3Ge)_2SiH_2$ (704 cm^{-1}) and "3" in $(H_3Ge)_3SiH$ (686 cm^{-1}), while asymmetrical Ge−H wagging vibrations have been identified as features "7" in $(H_3Ge)_2SiH_2$ (884 cm^{-1}), "6" in $(H_3Ge)_3SiH$ (883 cm^{-1}), and "2" in $(H_3Ge)_4Si$ (887 cm^{-1}). Finally, feature "8" in $(H_3Ge)_2SiH_2$ (930 cm^{-1}) is uniquely assigned as a symmetric H−Si−H bending mode and is not present in the other molecules. In summary, symmetric and anti-symmetric Ge−H wagging vibrations occur at approximately 790 and 885 cm^{-1} in all molecules, respectively, while symmetric Si−H wagging correlates with spectral features near 695 cm^{-1}. The remaining weak features have also been analyzed, and their detailed assignment will be presented elsewhere.

Film Growth. Initial deposition reactions of the $(H_3Ge)_xSiH_{4-x}$ compounds were conducted in a gas source MBE chamber with base pressure of 2×10^{-10} Torr. The Si(100) substrates were prepared for epitaxy by repeated flashing at 1240 °C to vaporize the native oxide layer. Film growth was obtained by exposing the substrate surface to the gaseous precursor at partial pressures in the range of 10^{-7} to 10^{-6} Torr. Under these conditions, the H_3GeSiH_3, $(H_3Ge)_2SiH_2$, $(H_3Ge)_3SiH$, and $(H_3Ge)_4Si$ compounds dissociated on the Si surface via complete H_2 elimination at 450, 400, 350, and 300 °C, respectively, to produce films at growth rates of 2−3 nm/min. RBS in random mode indicated film compositions of SiGe, $SiGe_2$, $SiGe_3$, and $SiGe_4$, respectively, in agreement with the elemental content of the Si/Ge framework of the corresponding precursors. The RBS channeled spectra showed that the Si and Ge atoms in the structure channeled remarkably well despite the low growth temperature, which is consistent with monocrystalline materials in epitaxial alignment with the Si substrate. As a representative example, Figure 4 compares RBS random and channeled spectra for a $SiGe_3$ film on Si(100). As in this case, in most samples the

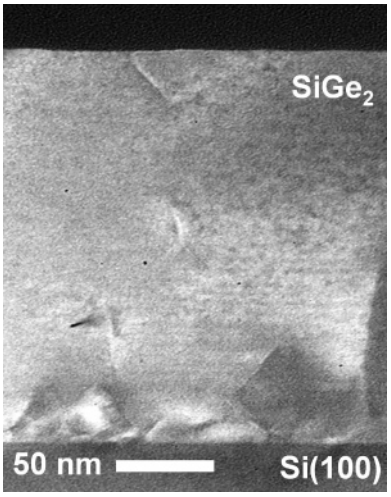

Figure 5. XTEM micrograph of a $SiGe_2$ layer grown on Si(100). The bulk of the threading dislocations is concentrated at the interface and does not propagate to the surface. In addition, the layer is highly uniform in thickness and displays an atomically smooth and continuous surface morphology.

ratio of the aligned versus the random peak heights (χ_{min}), which measures the degree of crystallinity across the layer, was relatively low, typically ranging from 30% at the interface to 7% near the surface. The decrease of the χ_{min} value across the layer thickness suggests that most of the defects are concentrated near the interface region. This was clearly established by cross-sectional transmission electron microscopy (XTEM). The bright field XTEM images in ⟨110⟩ projection show common threading dislocations propagating along the (111) lattice planes. Nevertheless, the bulk of these defects annihilated at 60° angles within 10 nm from the film interface (Figure 5). The upper portion of the film is relatively free of threading defects, particularly those penetrating to the top surface. In addition, phase and Z-contrast high-resolution XTEM images showed sharp and well-defined interfaces with perfectly epitaxial microstructures in which the (111) lattice planes of the film and the substrate are completely commensurate. The surface morphology of the films was examined by AFM scans. The films possess highly planar surfaces even in the 100−500-nm thickness range, which considerably exceeds the expected critical thickness. The AFM RMS values range between 0.5 and 1 nm for typical 25 μm × 25 μm areas. In addition, the surface planarity was found to be thermally stable up to 750 °C.

Raman and high-resolution XRD were used to investigate the structural, bonding, and strain properties of all films. In particular, the Raman spectra of the $SiGe_2$, $SiGe_3$, and $SiGe_4$ materials showed that the films are fully relaxed. X-ray reciprocal space maps of the (224) and (004) reflections were used to measure the lattice constants normal and parallel to the interface plane. These were virtually identical in most samples, indicating a lack of strain distortion from perfect cubic symmetry. In addition, the X-ray data indicated highly aligned heterostructures with mosaics spreads as low as 0.1°. In contrast to $SiGe_x$ ($x = 2, 3, 4$), the SiGe alloys possessed substantial residual strain. The X-ray reciprocal space map measurements showed an elongation along the "c" direction consistent with a tetragonal distortion. The calculated strain was in the 60−70% range. Remarkably, similar strain values were determined from Raman shifts of the Si−Si, Si−Ge, and Ge−Ge phonon modes.

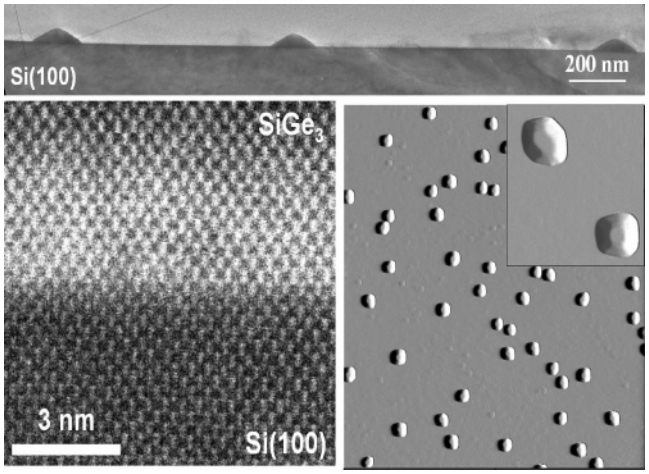

Figure 6. (Top panel) A bright field XTEM micrograph showing a set of highly coherent (no threading defects) $SiGe_3$ quantum dots of uniform size. (Left panel) High-resolution Z-contrast image of the interface region showing perfect epitaxial alignment as well as a sharp and uniform interface. (Right panel) AFM image showing an ensemble of dome-shaped islands with a narrow size distribution. Inset is an enlarged view of faceted islands.

Raman was used to investigate the distribution of strain in these SiGe layers, by measuring the phonon frequencies using laser lines with different penetration depths. The results showed that the Raman peaks did not change with depth, indicating that the strain does not vary across the layers. Collectively, the characterization of our Si−Ge materials revealed growth of crystalline, highly epitaxial, smooth, continuous, and uniform alloy layers with Ge-rich concentrations and uniformly stressed or strain-relaxed microstructures. The key to the successful synthesis of our films is the unprecedented[25] low growth temperatures that reduce surface mobility of the Si and Ge atoms and prevent mass segregation, thereby resulting in highly uniform compositional and strain profiles at the atomic level. In addition, the incorporation of the entire Si−Ge molecular core promotes the formation of exceptionally uniform bonding arrangements over the entire crystal, leading to relaxed films with planar surface morphology (no surface ripples).

The growth of Si−Ge materials via dehydrogenation of $(H_3Ge)_xSiH_{4-x}$ was investigated in the temperature range of 300−700 °C. In the high temperature regime, we observe exclusive growth of self-assembled islands, or quantum dots. Presumably these form spontaneously during the epitaxial growth of Si−Ge on Si to relieve the strain induced by the mismatch between the film and the substrate. In our experiments, the islands appear after the formation of a completely planar wetting layer ~3−5 monolayers thick. The morphology distribution and size of the islands were examined by AFM and XTEM. A representative AFM image of islands grown at 550 °C using $(H_3Ge)_2SiH_2$ is presented in Figure 6. The islands are primarily dome-shaped and reasonably uniform in size with an approximate density distribution of $\sim 3 \times 10^8$ cm^{-2}. The bright field XTEM micrographs showed ensembles of coherent islands with defect-free microstructure and with a narrow size distribution. The microstructural properties of the islands were explored via Z-contrast imaging performed on a JEOL 2010F. These experiments confirmed the presence of distinct islands grown on the substrate surface via a wetting layer of uniform thickness

(25) Kim, H.; Taylor, N.; Bramblett, T. R.; Greene, J. E. *J. Appl. Phys.* **1998**, *84*, 6372−6381.

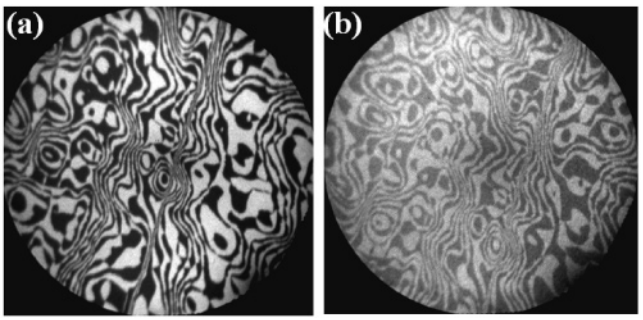

Figure 7. LEEM images of CVD of $SiGe_2$ on Si(100)−(2 × 1) at 350 °C over a field of view of 8 μm taken with the ($^1/_2$,0) diffraction beam such that the (2 × 1) and (1 × 2) terraces separated by single-height atomic steps alternate in contrast from dark to bright due to the rotation of the dimer reconstruction across a step. (a) Morphology of a clean surface. (b) Deposition of the first layer.

as shown for a representative sample produced by $(H_3Ge)_3SiH$. Note that in Z-contrast images the intensity is proportional to $Z^{1.7}$, and consequently the Ge-containing islands as well as the wetting layers appear considerably brighter than the underlying Si. Figure 6 is also representative of the most commonly found quantum dot microstructure showing a perfectly sharp and uniform interface. The highly coherent nature (no defects are observed) of the quantum dots grown by our method is confirmed by the Raman spectra, which show that the islands are highly strained, as expected due to the lattice mismatch of the dots with the substrate. We used RBS and electron energy loss spectroscopy (EELS) at 1.7 Å resolution to determine the dot stoichiometry and elemental homogeneity. The compositions of the islands were found to be $SiGe_2$, $SiGe_3$, and $SiGe_4$, reflecting the stoichiometries of the unimolecular precursors $(H_3Ge)_2SiH_2$, $(H_3Ge)_3SiH$, and $(H_3Ge)_4Si$, respectively, used for growth. EELS compositional profiles across the dots revealed remarkably uniform elemental distributions at the nanometer scale. An important point to make with regard to composition is that there is no apparent mixing of the elements across the interface as is typically observed when pure Ge islands are grown on Si at $T > 550$ °C. This type of Si interdiffusion from the substrate into Ge islands represents the most commonly reported method to form Si−Ge quantum dots on Si with Ge > 50 atom %. Unfortunately, interdiffusion of the elements in this case depletes the Si at the base of the islands to form a trench several nanometers in depth. In addition, the Si/Si−Ge dot interface is no longer distinct. A wide and blurred transition region with a graded composition develops across the original interface. Substantial gradients of concentration are also found in the vertical direction across the entire dot. Our single source approach circumvents these difficulties.

Growth Kinetics. The decomposition profiles of H_3GeSiH_3, $(H_3Ge)_2SiH_2$, $(H_3Ge)_3SiH$, and $(H_3Ge)_4Si$ to form the corresponding SiGe, $SiGe_2$, $SiGe_3$, and $SiGe_4$ layers were investigated using low energy electron microscpopy (LEEM). In particular, the activation energy with respect to H_2 desorption from the Si(100) surface was determined for each of the compounds by measuring the growth rate versus temperature for a single Si−Ge monolayer. Figure 7 shows LEEM images of a clean Si surface and the first full monolayer of $SiGe_2$ produced via deposition of $(H_3Ge)_2SiH_2$. The contrast reversal in the (2 × 1) and (1 × 2) terraces indicates a layer-by-layer growth. The average growth rate for the first layer as a function of temperature was measured, and activation energies were ex-

tracted from its temperature dependence. The data are consistent with first-order H_2 desorption kinetics and yield activation energies 1.7, 1.7, and 1.5 eV for $(H_3Ge)_2SiH_2$, $(H_3Ge)_3SiH$, and $(H_3Ge)_4Si$, respectively. For comparison, the activation energy of pure H_3GeGeH_3 (1.7 eV) was also determined using the same method. Note that these activation energies are remarkable similarity to that of H_3GeGeH_3. Furthermore, the activation energies are in good agreement with the values of 1.7 and 1.6 eV obtained previously for H_2 desorption from a pure Ge(100) surface.[26] It is interesting to note that our growth study of H_3GeSiH_3 in the LEEM gave an activation energy of 2.0 eV, which is intermediate to our measured value of digermane (1.7 eV) and that reported for disilane (2.3 eV).[27] The 2.0 eV value appears to be reasonable since H_3GeSiH_3 is essentially a compositional hybrid of H_3SiSiH_3 and H_3GeGeH_3 (i.e., $H_3SiSiH_3 + H_3GeGeH_3 \rightarrow 2\ H_3GeSiH_3$).

The activation energy results reveal that the decomposition kinetics of the series $(H_3Ge)_xSiH_{4-x}$ ($x = 2-4$) are remarkably similar to those of $(GeH_3)_2$ and suggest that these compounds are more reactive than either $(SiH_3)_2$ or GeH_3SiH_3. Accordingly, they represent a unique low-temperature source to Ge-rich $Si_{1-x}Ge_x$ alloys. The facile reactivity of $(H_3Ge)_2SiH_2$, $(H_3Ge)_3SiH$, and $(H_3Ge)_4Si$ pave the way to immediate development of SiGe semiconductors on specialty substrates able to endure low-temperature processing below 300 °C such as flexible displays.

Conclusions

We have described synthetic routes that provide the entire family of $(H_3Ge)_xSiH_{4-x}$ ($x = 1-4$) silicon−germanium hydrides with molecular formulas H_3GeSiH_3, $(H_3Ge)_2SiH_2$, $(H_3Ge)_3SiH$, and $(H_3Ge)_4Si$. A complete characterization of the products was conducted via a range of spectroscopic and analytical methods, and the data collectively confirm the proposed molecular compositions and tetrahedral structures in which a central Si atom is bonded directly to H and GeH_3 groups. The experimental results compare extremely well with DFT calculations of the spectroscopic and bonding properties of the molecules. The $(H_3Ge)_2SiH_2$, $(H_3Ge)_3SiH$, and $(H_3Ge)_4Si$ are isolated for the first time as volatile colorless liquids that display the necessary physical and chemical properties to be viable chemical vapor deposition sources. The previously known H_3GeSiH_3 gaseous analogue has been synthesized in practical high purity yields. Targeted deposition experiments of the compounds have been conducted via gas-source MBE to delineate the parameter space for growth of device quality films and quantum dots directly on silicon substrates. The films are obtained in the low-temperature range 300−450 °C and fulfill crucial requirements as suitable candidates for development of lattice-engineered "virtual substrates" on Si. Potential applications include integration of strained Si and Ge channel devices on silicon exhibiting extremely high electron and hole mobilities. In the high temperature range, depositions of the precursors yield assemblies of three-dimensional coherently strained islands (quantum dots) reflecting the stoichiometry of the precursor in all cases without any segregation of either Ge or Si.

Experimental Section

General. All manipulations were carried out under inert conditions using standard Schlenk and drybox techniques. Dry, air-free solvents were distilled from either anhydrous $CaCl_2$ or sodium benzophenone ketyl prior to use. Di-*n*-hexyl ether was dried and distilled from Na−K alloy prior to use. All NMR spectra were collected on an Varian INOVA 500 spectrometer operating at 500 MHz. Samples were dissolved in $CDCl_3$, and all nuclei were referenced either directly or indirectly to TMS or the residual solvent peak (7.24 ppm) unless specified otherwise.[28] IR spectra were recorded using a 10-cm gas cell with KBr windows. Elemental analyses were performed by Desert Analytics (Tucson, AZ). Gas chromatography mass spectrometry (GC−MS) spectra were obtained using a JEOL JMS-GC Mate II spectrometer (IE 45.4 eV). Trifluoromethane sulfonic acid (Alfa Aesar), di-*n*-hexyl ether (Alfa Aesar), nonafluorobutane-1-sulfonic acid (Aldrich), diphenylsilane (Gelest), triphenylsilane (Gelest), dichlorodiphenylsilane (Gelest), and semiconductor-grade germane (Voltaix, Inc.) were used as received. Phenylgermylsilane, phenylsilane, and silyl triflate were prepared according to literature procedures.[7,29,30] $KGeH_3$ was synthesized in either monoglyme or diglyme via a modified literature preparation using sodium−potassium (80% K) alloy. Both bis- and tris-(trifluoromethylsulfonyloxy)silane were synthesized according to the reported literature method.[31] Although synthetic methodologies for $H_xSi(SO_3CF_3)_{4-x}$ ($x = 1, 2$) and $Cl_2Si(SO_3CF_3)_2$ have been described in the literature, we found that these did not give the correct conditions leading to the target compounds in suitable yield and purity. Below we describe modified procedures to obtain these in pure form and quantitative yields in most cases.

$H_2Si(SO_3CF_3)_2$ and $HSi(SO_3CF_3)_3$. The preparation for $H_2Si(SO_3CF_3)_2$ and $HSi(SO_3CF_3)_3$ utilized reactions of the corresponding phenylsilanes with stoichiometric amounts of triflic acid. The synthesis of $HSi(SO_3CF_3)_3$ required heating of the reaction mixture under nitrogen at 60−80 °C for 12 h to achieve complete substitution of the phenyl groups. The synthesis of $H_2Si(SO_3CF_3)_2$ was carried out at ambient conditions. In both cases, the C_6H_6 byproduct was removed under vacuum, and the crude $H_2Si(SO_3CF_3)_2$ and $HSi(SO_3CF_3)_3$ products were purified by short path distillation at 49 °C/1.0 Torr and 45 °C/0.1 Torr, respectively, as colorless liquids in near-quantitative yields. The purity of each compound was checked by NMR spectroscopy.

$Cl_2Si(SO_3CF_3)_2$. HSO_3CF_3 (15.0 g, 100.0 mmol) was added dropwise to pure Cl_2SiPh_2 (12.0 g, 47.4 mmol) in a 200-mL flask over the course of 20 min, with continuous stirring, at 0 °C. The mixture was slowly warmed to 22 °C and stirred for 18 h and then distilled several times through a U-trap held at −25 °C. Pure $Cl_2Si(SO_3CF_3)_2$ was obtained as a clear liquid (10.7 g, 57% yield) and checked by ^1H NMR ($CDCl_3$) to confirm the absence of phenyl protons. ^{29}Si NMR (99.3 MHz, $CDCl_3$): δ −62.5. GC−MS: *m/z* 398.3 ($M^+ = Cl_2Si(SO_3CF_3)_2^+$), 363.8 ($M^+ - Cl$), 345.4 ($M^+ - Cl, F$), 324.0 ($M^+ - 2F$), 260.1 ($M^+ - 2CF_3$), 246.4 ($M^+ - SO_3CF_3$), 181.9 ($ClSO_3CF_3$), 149.9 ($SO_3CF_3^+$), 134.0 ($SO_2CF_3^+$), 99.9 ($SO_2Cl^+$, SO_3F^+).

$H_2Si(SO_3C_4F_9)_2$. Diphenylsilane (4.40 g, 23.9 mmol) was added dropwise, under N_2, to a sample of $HSO_3C_4F_9$ (14.33 g, 47.7 mmol) in a 50-mL flask at 0 °C. The flask was warmed to 22 °C, and the mixture was stirred for 2 h after which the C_6H_6 byproduct was removed in a vacuum to yield a colorless solid that was recrystallized from toluene at −20 °C. ^1H NMR (500 MHz, $CDCl_3$): δ 5.287 (s, $^1J_{SiH} = 318.4$ Hz, $Si-H_2$). ^{29}Si NMR (99.3 MHz, $CDCl_3$): δ −32.2. Anal. Calcd for $C_8F_{18}S_2O_6SiH_2$: C, 15.3; H, 0.03; F, 54.4. Found: C, 14.99; H, 0.78; F, 53.79. Mp = 39 °C. An $^1H-^{29}Si$ HMQC NMR spectrum showed that the ^1H resonance at 5.287 ppm was directly coupled to the ^{29}Si resonance at −32.2 ppm.

(26) (a) Eres, G.; Sharp, J. W. *J. Vac. Sci. Technol., A* **1993**, *11*, 2463−2471. (b) Bramblett, T. R.; Lu, Q.; Lee, N. E.; Taylor, N.; Hasan, M. A.; Greene, J. E. *J. Appl. Phys.* **1995**, *77*, 1504−1513.
(27) Takahashi, J.; Utsumi, Y.; Akazawa, H.; Kawashima, I.; Urisu, T. *Appl. Phys. Lett.* **1991**, *58*, 2776−2778.
(28) Harris, R. K.; Becker, E. D.; Cabral De Menezes, S. M.; Goodfellow, R.; Granger, P. *Pure Appl. Chem.* **2001**, *73*, 1795−1818.
(29) Zech, J.; Schmidbauer, H. *Chem. Ber.* **1990**, *123*, 2087−2091.
(30) Olah, G. A.; Hussain, A.; Gupta, B. F. B.; Salem, G. F.; Narang, S. C. *J. Org. Chem.* **1981**, *46*, 5212−5214.
(31) Uhlig, W.; Tzschach, A. *J. Organomet. Chem.* **1989**, *378*, C1−C5.

$HSi(SO_3C_4F_9)_3$. Triphenylsilane (2.84 g, 10.9 mmol) was added under N_2 to pure $HSO_3C_4F_9$ (10.20 g, 34.0 mmol) in a 50-mL flask at 0 °C. The mixture was warmed to 22 °C and stirred for 2 h, after which the C_6H_6 byproduct was removed in a vacuum. The colorless liquid was heated at 95 °C for 24 h, and the additional byproduct C_6H_6 was removed under vacuum. The product was purified by extracting with CH_2Cl_2. Pure $HSi(SO_3C_4F_9)_3$ was obtained as a colorless liquid in nearly quantitative yield. ^{1}H NMR (500 MHz, $CDCl_3$) δ 5.520 (s, $^1J_{SiH}$ = 414.7 Hz, Si−H). ^{29}Si NMR (99.3 MHz, $CDCl_3$) δ −76.1. Anal. Calcd for $C_{12}F_{27}S_3O_9SiH$: C, 15.56; H, 0.01; F, 55.38. Found: C, 15.57; H, 0.39; F, 55.29. An ^{1}H−^{29}Si HMQC NMR spectrum showed that the ^{1}H resonance at 5.520 ppm was directly coupled to the ^{29}Si resonance at −76.1 ppm.

H_3GeSiH_3. A solution of $KGeH_3$ (4.00 g, 3.49 mmol) in diglyme (45 mL) was slowly added over the course of 45 min to a toluene solution (35 mL) of $H_3Si(SO_3CF_3)$ (9.43 g, 5.24 mmol) in a 250-mL flask with stirring at −60 °C. The procedure involved the addition of several drops of $KGeH_3$/diglyme to the reaction flask with vigorous stirring and subsequent trapping of the product through −78 and −196 °C traps under static vacuum. This procedure was repeated until all of the $KGeH_3$ had been added. The reaction flask was slowly warmed to 22 °C with continuous pumping through −78 and −196 °C traps for 1 h. Gas-phase IR revealed the presence of diglyme and toluene (−78 °C trap) and H_3SiGeH_3, SiH_4, and GeH_4 (−196 °C trap). The contents of the −196 °C trap were redistilled through U-traps held at −135 and −196 °C to collect pure H_3GeSiH_3 (−135 °C) in 35% yield. Significant amounts of SiH_4 and GeH_4 were also found in the −196 °C trap.

$(H_3Ge)_2SiH_2$. Method A. A solution of $H_2Si(SO_3C_4F_9)_2$ (8.80 g, 14.00 mmol) in di-*n*-hexyl ether (40 mL) was added dropwise to a solution of $KGeH_3$ (3.5 g, 30.4 mmol) in di-*n*-hexyl ether (30 mL) at −35 °C over the course of 35 min in a 250-mL flask. The mixture was warmed to 22 °C and stirred for ∼20 h. The volatiles were passed through a series of U-traps held at −35 and −196 °C under dynamic vacuum. The reaction flask was heated slowly to 43 °C while being pumped through −35 and −196 °C U-traps for 5 h. The −35 °C trap contained pure solvent. The contents of the −196 °C trap were redistilled through a series of U-traps held at −78, −130, and −196 °C. Pure $(H_3Ge)_2SiH_2$ was collected in the −78 °C trap (1.5 g, 60%). The −130 °C trap contained 0.311 g of pure H_3GeSiH_3, and the −196 °C trap contained traces of GeH_4 and SiH_4. Vapor pressure: 55 Torr (22 °C), 17 Torr (0 °C). IR (gas, cm^{-1}): 2152 (m), 2074 (vs), 2010 (w), 927 (w), 917 (w), 883 (w), 803 (s), 769 (vw), 723 (vw), 696 (vs), 649 (vw), 641 (vw), 547 (vw), 515 (vw), 424 (vw), 330 (vw). ^{1}H NMR (500 MHz, $CDCl_3$): δ 3.394 (sept, J = 4 Hz, 2H, Si−H_2), δ 3.110 (t, J = 4 Hz, 6H, Ge−H_3). ^{29}Si NMR (99.3 MHz, $CDCl_3$): δ −102.5. EIMS (*m*/*e*): isotopic envelopes centered at 174 ($M^+ - nH$), 148 ($Ge_2H_{6-x}^+$), 106 ($H_3GeSiH_3^+$), 75 (GeH_4^+), 31 (SiH_4^+).

Method B. A liquid sample of $H_2Si(SO_3CF_3)_2$ (2.72 g, 8.3 mmol) was added slowly to a solution of $KGeH_3$ (2.37 g, 20.7 mmol) in di-*n*-hexyl ether (25 mL) at −25 °C. The mixture was warmed to 22 °C and stirred for 24 h, after which the volatiles were collected under dynamic vacuum in traps held at −30 and −196 °C. The reaction flask was then heated to 43 °C for 1−2 h while opened to the −30 and −196 °C traps. The −30 °C trap collected pure solvent. The contents of the −196 °C trap were distilled through a series of U-traps cooled to −20, −78, and −196 °C, which collected solvent, $(H_3Ge)_2SiH_2$, and a mixture of GeH_4, SiH_4, and H_3SiGeH_3, respectively. The yield of $(H_3Ge)_2SiH_2$ was 0.220 g (15%). We also conducted this reaction in inert high boiling point solvents such as dry *n*-decane at 0 °C using essentially the same conditions. The main product was $(H_3Ge)_2SiH_2$, which was isolated in approximately 10% yield. Small amounts of H_3GeSiH_3, SiH_4, and GeH_4 were also produced.

$(H_3Ge)_3SiH$. A liquid sample of $HSi(SO_3CF_3)_3$ (4.10 g, 8.6 mmol) was added dropwise to an ether solution (40 mL) of $KGeH_3$ (4.0 g, 35 mmol) at −35 °C in a 100-mL flask. The reaction flask was warmed to 22 °C, and the mixture was stirred for 5 h. The volatiles, including solvent and products, were distilled under dynamic vacuum into traps held at −40 °C ($(H_3Ge)_3SiH$ and trace ether), −78 °C (ether and a trace $(H_3Ge)_2SiH_2$), and −196 °C (ether and trace GeH_4). The contents of the −40 °C trap were separated by fractional distillation to obtain pure $(H_3Ge)_3SiH$ (0.645 g, 30% yield). The vapor pressure of $(H_3Ge)_3SiH$ is 10 Torr at 22 °C. IR (gas, cm^{-1}): 2132 (m), 2071 (vs), 2010 (w), 922 (vw), 881 (w), 788 (vs), 745 (vw), 680 (s), 634 (vw), 606 (w), 514 (vw), 409(vw). ^{1}H NMR (500 MHz, $CDCl_3$, 5 °C): δ 3.410 (dec, J = 4 Hz, 1H, Si−H), δ 3.294 (d, J = 4 Hz, 9H, Ge−H_3). ^{29}Si NMR (99.3 MHz, $CDCl_3$, 5 °C) δ −112.7 (s). GC−MS: *m*/*z* 255−238 ($SiGe_3H_x^+$), 230−213 ($Ge_3H_x^+$), 185−170 ($SiGe_2H_x^+$), 154−140 ($Ge_2H_x^+$), 109−100 ($SiGeH_x^+$), 77−71 (GeH_x^+).

An alternate synthesis of $(H_3Ge)_3SiH$ involving the reaction of $HSi(SO_3C_4F_9)_3$ with $KGeH_3$ under conditions virtually identical to those described above gave a comparable yield.

$(H_3Ge)_4Si$. A liquid sample of $Cl_2Si(SO_3CF_3)_2$ (2.40 g, 6 mmol) was added at −45 °C to a mixture of $KGeH_3$ (2.98 g, 26 mmol) in 50 mL of diethyl ether. (The pressure in the reaction assembly was reduced to 300 Torr during the addition of $Cl_2Si(SO_3CF_3)_2$.) The flask was then warmed to 22 °C, and the mixture was stirred at 22 °C for 2 h. The volatiles were subsequently collected in a U-trap held at −196 °C under dynamic vacuum. The contents of the −196 °C trap were redistilled through a −45 °C trap to remove the ether and collect a mixture of $(H_3Ge)_3SiH$ and $(H_3Ge)_4Si$. Final fractionation was accomplished by distillation through U-traps cooled to −10 and −45 °C. Gas-phase IR revealed $(GeH_3)_4Si$ (−10 °C trap) at approximately 5% yield a small amount of $(H_3Ge)_3SiH$ (−45 °C trap) and copious amounts of germane. No H_3GeGeH_3 was observed, indicating that the compound does not decompose via digermane formation. Vapor pressure of $(H_3Ge)_4Si$: 1 Torr (22 °C). IR (gas, cm^{-1}): 2130 (vw), 2072 (s), 2062 (s), 2020 (vw), 881 (vw), 777 (vs), 680 (vw), 632 (vw). ^{1}H NMR (500 MHz, $CDCl_3$): δ 3.437 (s, Ge−H). ^{29}Si NMR (99.3 MHz, $CDCl_3$): δ −127.6. GC−MS: *m*/*z* 328−318 ($SiGe_4H_x^+$), 255−238 ($SiGe_3H_x^+$), 230−213 ($Ge_3H_x^+$), 185−170 ($SiGe_2H_x^+$), 154−140 ($Ge_2H_x^+$), 109−100 ($SiGeH_x^+$), 77−71 (GeH_x^+).

Synthesis of $(H_3Ge)_2SiH_2$ via $H_3GeSiH_2(SO_3CF_3)$. $H_3GeSiH_2(SO_3CF_3)$. Neat HSO_3CF_3 (0.645 g, 4.3 mmol) was added slowly to $PhSiH_2GeH_3$ (0.784 g, 4.3 mmol) at −35 °C and stirred for 30 min. The mixture was warmed to 22 °C, and the contents were distilled under vacuum through U-traps held at −25 and −196 °C. Pure colorless $H_3GeSiH_2(SO_3CF_3)$ was obtained in the −25 °C trap (0.756 g, 72%) (vapor pressure ≈ 3.0 Torr at 22 °C). The −196 °C trap contained C_6H_6 and a small amount of H_3GeSiH_3. IR (gas, cm^{-1}): 2194 (w), 2155 (s), 2071 (vs), 1425 (m), 1253 (w), 1225 (ms), 1158 (m), 1077 (s), 964 (ms), 951 (ms), 883 (s), 863 (ms), 844 (w), 792 (s), 763 (vs), 690 (vw), 625 (w), 467 (vw), 434 (vw), 355 (vw). ^{1}H NMR (500 MHz, $CDCl_3$): δ 5.430 (q, 2H, Si−H_2), 3.514 (t, 3H, Ge−H_3). ^{13}C NMR (125.7 MHz, $CDCl_3$): δ 118 (q, 1C, CF_3). ^{19}F NMR (470.5 MHz, $CDCl_3$): δ −76.34 (s, 3F). The integrated ^{1}H peak ratio between resonances assigned to Si−H and Ge−H was found to be 2:3, respectively. A 2D ^{1}H COSY NMR spectrum showed cross-peaks that correlated to Si−H and Ge−H resonances at 5.430 and 3.514 ppm, respectively, indicating the H−Si−Ge−H connectivity.

$(H_3Ge)_2SiH_2$. Solid $KGeH_3$ (1.70 g, 14.8 mmol) was added to a solution (20 mL) of $H_3GeSiH_2(SO_3CF_3)$ (2.8 g, 11.0 mmol) in *n*-decane at −25 °C. The mixture was stirred at 22 °C for 1 h. The volatiles were fractionally distilled through a series of U-traps held at −25, −78, and −196 °C, which collected small amounts solvent, $(H_3Ge)_2SiH_2$, and a mixture of GeH_4, SiH_4, and H_3SiGeH_3, respectively.

Acknowledgment. We thank Dr. Hord (CRI, ASU) for assistance in the mass spectrometric measurements, and Dr. Crozier for assistance in Z-contrast TEM. The work was supported by grants from the National Science Foundation (DMR-0221993, DMR-0303237) and the U.S. Army Research Office (ARO). We acknowledge the use of computing resources in the Goldwater Materials Visualization Facility at Arizona State University.

JA051411O